Articles

Efficient Polymer Solar Cells Based on M3EH−PPV

Thomas Kietzke,*,† Hans-Heinrich Hörhold,‡ and Dieter Neher†

Institute of Physics, University of Potsdam, Am Neuen Palais 10, 14469 Potsdam, Germany, and Institute of Organic Chemistry and Macromolecular Chemistry, Humboldtstrasse 10, University of Jena, 07743 Jena, Germany

Received January 21, 2005. Revised Manuscript Received September 25, 2005

We report on polymer blend solar cells with an external quantum efficiency of more than 30% and a high overall energy conversion efficiency (ECE) under white light illumination (100 mW/cm^2) of up to 1.7% using a blend of M3EH−PPV (poly[2,5-dimethoxy-1,4-phenylene-1,2-ethenylene-2-methoxy-5-(2-ethylhexyloxy)−(1,4-phenylene-1,2-ethenylene)]) and CN−ether−PPV (poly[oxa-1,4-phenylene-1,2-(1-cyano)ethenylene-2,5-dioctyloxy-1,4-phenylene-1,2-(2-cyano)ethenylene-1,4-phenylene]). We attribute these high efficiencies to the formation of a vertically composition graded structure during spin coating. Photoluminescence measurements performed on the blend layers indicated the formation of exciplexes between both types of polymers, which we propose to be one factor preventing even higher efficiencies.

Introduction

On the route toward inexpensive renewable energy sources, research on organic solar cells has seen increasing interests over the past few years. Several approaches have been explored, the most promising are relying on small molecules[1,2] and conjugated polymers.[3−6] Currently there is a head to head race going on between both approaches with respect to achieved efficiencies. The easier processing may finally turn the balance in favor of polymers. Unlike for small molecules, the preparation of thin polymer layers does not require highly sophisticated processing like vacuum sublimation. Thin polymer layers can be deposited by less complex methods such as spin coating, screen printing, spray coating, or ink jet printing.

It is well-documented that energy conversion efficiencies of solar cells made with only one type of conjugated polymers (or small molecule) are quite low. This is due to the rather high exciton binding energy (200−500 meV) found in semiconducting organic materials. Solar cells based on a heterojunction between hole and electron transporting polymers have shown performances superior to single-component devices.[7−9] By using the heterojunction approach, photogenerated excitons in the polymer layer can be efficiently dissociated into free carriers at the interface. However, due to an exciton diffusion length in disordered organic layers in the range of 10 nm only, the spatial extent of the individual phases must be on a nanometer scale. A heterojunction can be employed in several ways. The most straightforward approach is the preparation of a double layer either by laminating techniques,[7,10] by evaporation, or by spin coating a second layer on top of the first one, resulting in a more or less diffused bilayer structure.[11−13] An alternative method is the preparation of a polymer blend by spin coating a solution containing both polymers.[3,8] Due to the low entropy of mixing for polymers, blending two different polymers will generally lead to a phase-separated structure. These heterojunctions formed in the bulk lead to an increased interfacial area resulting in a much better exciton dissociation probability compared with a sharp double layer structure.

Despite the lower probability for excitons to reach the interface, the highest energy conversion efficiencies (ECE) for polymer−polymer heterojunction solar cells were demonstrated for double-layer devices. These devices were

---

* To whom correspondence should be addressed. E-mail: kietzke@rz.uni-potsdam.de.
† University of Potsdam.
‡ University of Jena.

(1) Xue, J.; Uchida, S.; Rand, B. P.; Forrest, S. R. *Appl. Phys. Lett.* **2004**, *84*, 3013−3015.
(2) Xue, J.; Uchida, S.; Rand, B. P.; Forrest, S. R. *Appl. Phys. Lett.* **2004**, *85*, 5757−5759.
(3) Brabec, C. J.; Sariciftci, N. S.; Hummelen, J. C. *Adv. Funct. Mater.* **2001**, *11*, 15−26.
(4) Padinger, F.; Rittberger, R.; Sariciftci, N. S. *Adv. Funct. Mater.* **2003**, *13*, 1−4.
(5) Wienk, M. M.; Kroon, J. M.; Verhees, W. J. H.; Knol, J.; Hummelen, J. C.; Van Hall, P. A.; Janssen, R. A. J. *Angew. Chem., Int. Edit.* **2003**, *42*, 3371−3375.
(6) Ma, W.; Yang, C.; Gong, X.; Lee, K.; Heeger, A. J. *Adv. Funct. Mater.*, **2005**, *15*, 1617−1622.
(7) Granstrom, M.; Petritsch, K.; Arias, A. C.; Lux, A.; Andersson, M. R.; Friend, R. H. *Nature* **1998**, *395*, 257−260.
(8) Yu, G.; Gao, J.; Hummelen, J. C.; Wudl, F.; Heeger, A. J. *Science* **1995**, *270*, 1789−1791.
(9) Yu, G.; Heeger, A. J. *J. Appl. Phys.* **1995**, *78*, 4510−4515.
(10) Barker, J. A.; Ramsdale, C. M.; Greenham, N. C. *Phys. Rev. B* **2003**, *67*, 075205-075201-075209.
(11) Chen, L. C.; Godovsky, D.; Inganas, O.; Hummelen, J. C.; Janssens, A. J.; Svensson, M.; Andersson, M. R. *Adv. Mater.* **2000**, *12*, 1367−1370.
(12) Jenekhe, S. A.; Yi, S. *Appl. Phys. Lett.* **2000**, *77*, 2635−2637.
(13) Inganas, O.; Roman, L. S.; Zhang, C.; Johansson, D. M.; Anderson, J. L.; Hummelen, J. C. *Synth. Met.* **2001**, *121*, 1525−1528.

10.1021/cm050148n CCC: $30.25

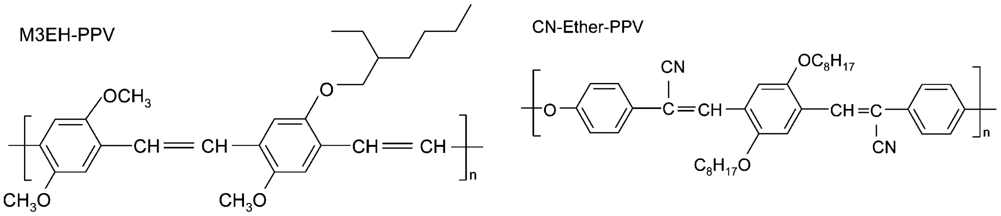

Figure 1. Chemical structures of M3EH−PPV and CN−ether−PPV.

produced either by laminating a polythiophene derivative (POPT) with a cyano-substituted poly(*p*-phenylene vinylene) (MEH−CN−PPV) as electron acceptor (ECE = 1.9%)[7] or by PPVs covered with a thin layer of polybenzimidazobenzophenanthroline ladder polymers (BBL; ECE = 1.5%).[14] However, the laminating technique still has to prove its applicability for large area devices while BBL is deposited from a strong acid making it less desirable for mass production.

In contrast, blends of an electron-donating and an electron-accepting polymer could not achieve the efficiencies obtained with the double-layer approach so far. Up to now the highest energy conversion efficiency of a pure polymer blend device was 1%, reported by using a blend of the copolymer M3EH−PPV[15] (poly[2,5-dimethoxy-1,4-phenylene-1,2-ethenylene-2-methoxy-5-(2-ethylhexyloxy)−(1,4-phenylenevinylene-1,2-ethenylene)]) and CN−ether−PPV (poly[oxa-1,4-phenylene-1,2-(1-cyano)ethenylene-2,5-dioctyloxy-1,4-phenylene-1,2-(2-cyano)ethenylene-1,4-phenylene])[16] (for the chemical structures see Figure 1).[17] Even higher efficiencies were published when replacing the electron-accepting polymer with fullerenes or their derivatives. Here, the blend structures currently outperform the double-layer structures with respect to energy conversion efficiencies. Whereas double-layer devices with poly(2-methoxy-5-(3′,7′-dimethyloctyloxy)-1,4-phenylenevinylene) (MDMO−PPV) and a [b,b]-phenyl-Cbl-butyric-acid-methyl-ester (PCBM) electron-accepting layer show rather low energy efficiencies of less than 0.5% [11,13] PCBM rich blends with polythiophenes (PT) or PPV derivatives were reported to yield efficiencies of up to 5% under solar irradiation.[4−6,18] However, the open-circuit voltage of a polymer−PCBM based device is typically limited to 0.8 V, a value much smaller compared to the 1.35 V reached for M3EH−PPV:CN−ether−PPV devices. This higher voltage is due to the smaller offsets of the HOMO (highest occupied molecular orbital) and LUMO (lowest unoccupied molecular orbital) levels of both polymers; thus less energy is lost when the photoexcited electron transfers from M3EH−PPV to the CN−ether−PPV molecule. (M3EH−PPV: HOMO, −5.3 eV; LUMO, −2.9 eV. CN−ether−PPV: HOMO, −6.05 eV; LUMO, −3.35 eV).

Here we discuss efficient solar cells based on M3EH−PPV as the electron-donator and CN−ether−PPV as the electron accepting component in more detail regarding the relationship between the layer structure and the electronic properties. M3EH−PPV can be considered a strictly alternating copolymer based on soluble MEH−PPV and insoluble 2,5-dimethoxy-PPV subunits. We compare the performance of devices prepared from a polymer blend and two-layer devices with respect to the spectral characteristics, the quantum efficiency, fill factor, and energy conversion efficiencies.

Experimental Section

Preparation. In the first step, an approximately 50 nm thin layer of poly(ethylene−dioxythiophene) doped with polystyrene sulfonic acid (PEDOT:PSS) was spin-coated at 2400 rpm onto commercially available glass substrates covered with indium−tin oxide (ITO, 13 Ω/square). Then, the PEDOT:PSS films were dried on a hot plate under nitrogen atmosphere for 30 min at 170 °C (transmission glass/ITO/PEDOT > 90% from 380 to 650 nm). For the blend devices we found that direct mixing of the low soluble copolymer M3EH−PPV with CN−ether−PPV in chlorobenzene led to the formation of small aggregates in solution. Homogeneous blend layers could be obtained by mixing M3EH−PPV with the desired amount of chlorobenzene and additional ultrasonication for about 1 h, until a clear solution was obtained. Then, CN−ether−PPV was added and the spin-coated layers were annealed in nitrogen atmosphere at 110 °C for 40 min. The devices were completed by evaporating a 25 nm Ca layer protected by 100 nm Al or by evaporating 10 nm of Au to obtain semitransparent electrodes at a base pressure of 2×10^{-6} mbar. The effective solar cell area as defined by the geometrical overlap between the bottom ITO electrode and the top cathode was 0.25 cm^2. All device preparation and characterization were performed under nitrogen atmosphere.

Device Characterization. The external quantum efficiency (IPCE) as a function of wavelength was measured with an Oriel 150 W Xe-lamp in combination with an Oriel Cornerstone 260 monochromator. The number of photons incident on the device was calculated for each wavelength by using a calibrated Si-diode as reference. *I(V)* characteristics were recorded with a Keithley 2400 source/measure-unit under illumination with a Steuernagel solar simulator at a light power density of 100 mW/cm^2. The white light power was measured with a Gentec pyroelectric power meter.

Optical Spectroscopy. Absorption spectra were recorded with a Perkin-Elmer UV-VIS spectrometer. All spectra were corrected for the transmission of the uncoated glass substrates.

Fluorescence spectra were measured with a Perkin-Elmer LS 55 luminescence spectrometer. The samples were irradiated at an incident angle of 60° onto the front of the sample, and the emission was recorded in reflection at an angle of 30°. For both measurements, areas of ca. 10 mm^2 were analyzed, which are representative for the whole sample area.

Results and Discussion

To compare the spectral response of different solar cells, the external quantum efficiency or incident-photon-to-converted-electron efficiency (IPCE) is widely used. This

---

(14) Alam, M. M.; Jenekhe, S. A. *Chem. Mater.* **2004**, *16*, 4647−4656.
(15) Pfeiffer, S.; Hörhold, H.-H. *Macromol. Chem. Phys.* **1999**, *200*, 1870−1878.
(16) Tillmann, H.; Hörhold, H.-H. *Synth. Met.* **1999**, *101*, 138−139.
(17) Breeze, A. J.; Schlesinger, Z.; Carter, S. A.; Hörhold, H.-H.; Tillmann, H. *Sol. Energy Mater. Sol. Cells* **2004**, *83*, 263−271.
(18) Rispens, M. T.; Meetsma, A.; Rittberger, R.; Brabec, C. J.; Sariciftci, N. S. *Chem. Commun.* **2003**, *17*, 2116−2118.

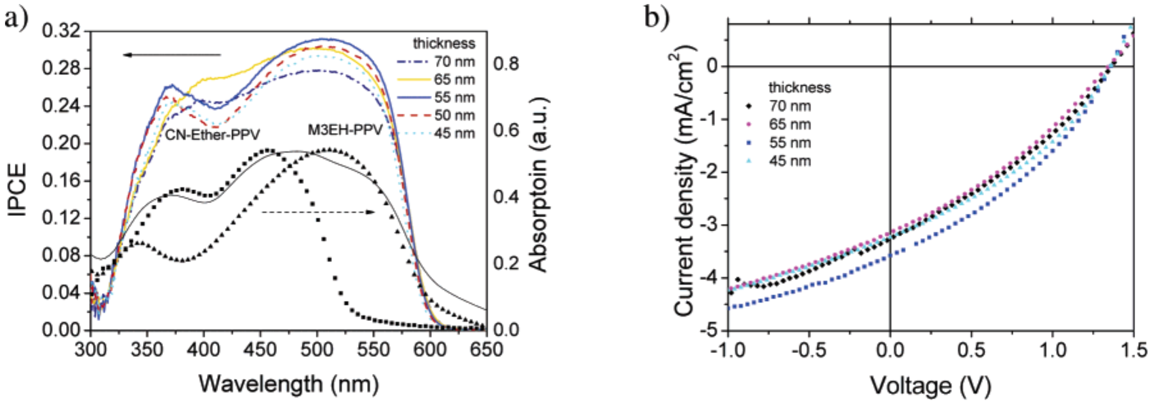

Figure 2. Characteristics of solar cells based on M3EH−PPV:CN−ether−PPV blends (1:1 ratio by mass) for different thicknesses of the active layer after annealing at 110 °C. (a) Comparison of the external quantum efficiencies (IPCE) and the absorption spectra of CN−ether−PPV (squares) and M3EH−PPV (triangles) of the blend layer (black line). (b) *I*(*V*) characteristics under white light illumination at an intensity of 100 mW/cm^2.

efficiency can be calculated by IPCE = $hcI_{SC}/e\lambda P_{light}$, where λ is the incident wavelength, I_{SC} the short circuit current per area, e the elementary charge, h the Planck constant, c the speed of light, and P_{light} is the incident light power per area.

As shown by Figure 2, solar cells based on a blend of M3EH−PPV and CN−ether−PPV (ratio 1:1 by mass) exhibited external quantum efficiencies of up to 31%. Annealing the layers at 110 °C prior to evaporation of the electrodes led to a significant increase in device efficiency and to a red shift of the long-wavelength "shoulder". This effect is also observed in the absorption spectra of pure M3EH−PPV layers before and after annealing (see Figure 8). We attribute this shift as well as the improved efficiency of the solar cells to a better ordering of the chains in the M3EH−PPV phase after the annealing step. The thicknesses of the active layers were varied in the range of 45 to 70 nm by changing the spinning speed. Quite surprisingly, changing the layer thickness led to only small changes in quantum efficiency. The maximum IPCE was found to be 31% at 508 nm for a 55 nm thick blend layer. Surprisingly this wavelength is close to the absorption maximum of M3EH−PPV and not at 480 nm where the blend layer has its maximum absorption. In fact, for wavelengths larger than 450 nm, the IPCE spectrum is clearly dominated by the M3EH−PPV absorption. Only thicker devices show a pronounced contribution around 400 nm where the CN−ether−PPV absorbs, but the overall efficiency of these devices is slightly smaller.

All devices exhibited comparable open-circuit voltages of around 1.36 V but differed slightly in the fill factor (FF). The FF dropped from 35.4% for a 40 nm thick layer to 32.0% for a 65 nm layer. This can be explained by the hindered charge carrier transport or smaller internal field in thicker devices. The 55 nm thick device exhibited the best efficiency under white light illumination at 100 mW/cm^2, yielding an energy efficiency of 1.7% (FF, 35.43%; I_{sc} = 3.57 mA; V_{oc} = 1.36 V). This is the highest value reported so far for solar cells based on polymer−polymer blends.

To evaluate if bimolecular recombination processes are limiting the device efficiency, intensity dependent measurements were performed. In the case in which bimolecular recombination constitute the main loss channel, the short-circuit current should exhibit a sublinear dependence on the light intensity. Alternatively, if the recombination of initially formed electron−hole pairs are limiting the device efficiency, the short-circuit current should scale linearly with the light intensity.[19]

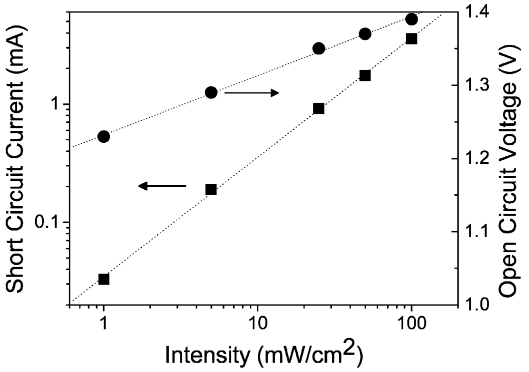

Figure 3. Dependence of the short-circuit current (squares) and open-circuit voltage (circles) on the light intensity for a 55 nm thick M3EH−PPV:CN−ether−PPV blend device.

As shown in the double-logarithmic plot in Figure 3, the short-circuit current scales linearly with light intensity (slope $\alpha = 1.01 \pm 0.02$). The linear dependence of the short-circuit current on the light intensity indicates that the charge carrier losses are due to monomolecular (exciton or geminate pair) recombination processes. This shows that the rate for biomolecular recombination is sufficiently slow compared to the charge transport of most of the photogenerated charges to the electrodes. No fundamental differences in this behavior could be found by varying the layer thickness between 45 and 70 nm. The open-circuit voltage increases by 0.080 ± 0.002 V per decade in intensity which is the same dependence as that reported for laminated bilayer devices of polyfluorene based solar cells.[20]

The pronounced contribution of M3EH−PPV to the IPCE spectrum can be explained under the assumption that a vertically composition graded layer is formed upon evaporation of the solvent. This results in a M3EH−PPV rich region close to the ITO:PEDOT:PSS layer where the light intensity and thus the exciton generation is largest since all devices

---

(19) Nelson, J. *Phys. Rev. B* **2003**, *67*, 155209.

(20) Ramsdale, C. M.; Bache, I. C.; MacKenzie, J. D.; Thomas, D. A.; Arias, A. C.; Donald, A. M.; Friend, R. H.; Greenham, N. C. *Physica E* **2002**, *14*, 268−271.

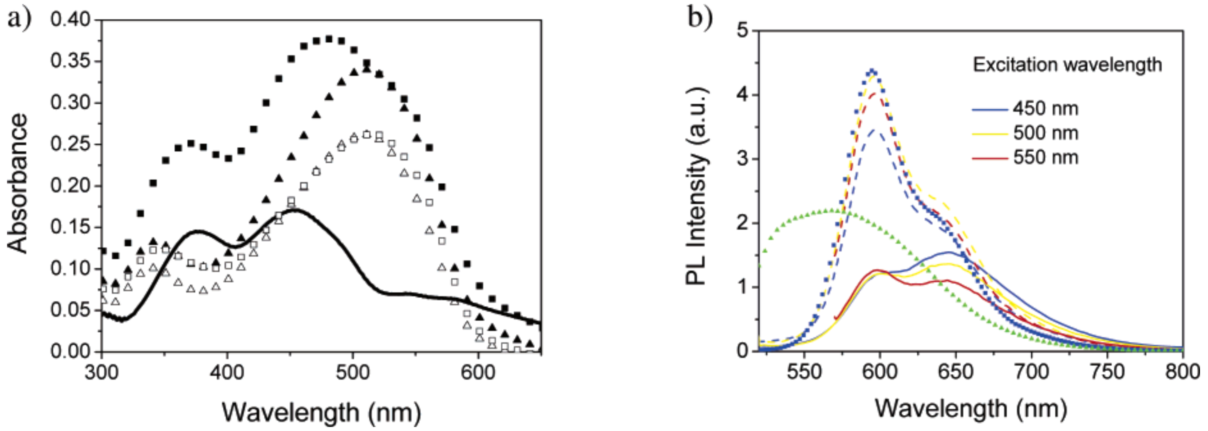

Figure 4. (a) Absorbance of a M3EH−PPV:CN−ether−PPV blend layer coated at 1800 rpm (squares) and of a pure M3EH−PPV layer (triangles) on ITO/PEDOT. The spectra are recorded before (solid symbols) and after (open symbols) rinsing with xylene. In addition, the difference in absorbance before and after washing the blend layer is plotted (solid line). (b) Photoluminescence spectra of the annealed blend layer measured at different excitation wavelengths before (solid line) and after washing (dashed line) with xylene. For comparison, the photoluminescence spectra of a pure M3EH−PPV layer (solid squares) and of a pure CN−ether−PPV layer (solid triangles) are shown.

were illuminated from the ITO side. We propose that due to the much lower solubility of M3EH−PPV compared to CN−ether−PPV in chlorobenzene, M3EH−PPV precipitates first during evaporation of the solvent in the spin-coating process. To prove our assumption, we washed the blend device with xylene, which preferentially dissolves the CN−ether−PPV compound and compared the absorbance and photoluminescence before and after the washing step. As shown in Figure 4a the absolute value of the absorbance of the blend layer dropped considerably after the washing step, and the shape of the spectrum after washing resemble fully the M3EH−PPV absorbance. This suggests that nearly all CN−ether−PPV but only a small fraction of M3EH−PPV was dissolved. As a reference also a pure M3EH−PPV layer was washed with xylene. This time the absorbance dropped by approximately 25%. Repeating the washing step did not reveal any further reduction in absorbance. This indicates that M3EH−PPV contains a fraction which is soluble in xylene. The layer thicknesses of all investigated blend layers dropped to less than half of the original values after washing with xylene. Concurrently, an increase in photoluminescence is also observed after the washing step.

Note that the emission spectrum of the blend layer exhibits a photoluminescence peak around 650 nm, which cannot be explained by an inner filter effect (Figure 4b). This feature is neither present in the spectra of the pure film nor in the blend layer after washing. Varying the excitation wavelength from 450 nm (excitation mostly of CN−ether−PPV) to 550 nm (excitation solely of M3EH−PPV) does not significantly change the strength of this long-wavelength contribution. In an as-prepared blend film the peak is better resolved and the 594 nm contribution of M3EH−PPV is nearly completely suppressed.

On the basis of comparable results for donor−acceptor blends of polyfluorene derivatives and first time-resolved measurements showing a significant increased fluorescence lifetime for the emission at 650 nm compared to the 600 nm emission, we attribute this peak to the formation of an exciplex between M3EH−PPV and CN−ether−PPV.[21] This idea may answer the question why, despite the fact that more than 95% of the excitons generated on M3EH-PPV are quenched in the presence of CN-ether-PPV, the external quantum efficiency of the device is only 30%. It is proposed that after dissociation of the excitons, no free charge carriers but bound polaron pairs (geminate pairs) are formed. These polaron pairs either may dissociate into free charge carriers, may be lost due to nonradiative decay channels or via formation of exciplexes. The probability for the formation of free charge carriers increases at higher fields, which may be the reason for the rather linear *I*(*V*) characteristics at negative voltages. Details on the time-resolved measurements are the subject of a separate publication.

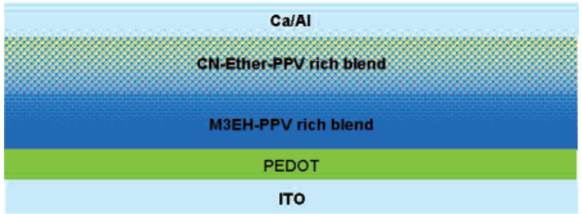

Figure 5. Proposed vertical composition gradient of the M3EH−PPV: CN−ether−PPV blend. Due to the lower solubility a M3EH−PPV rich phase (blue) is formed on the PEDOT layer incorporating a minor fraction of CN−ether−PPV upon evaporation of the solvent.

The shape of the emission spectrum after washing with xylene is completely dominated by the emission of M3EH−PPV, and the photoluminescence intensity reaches around two-thirds of the expected intensity for a neat M3EH−PPV film. Together with the results of the absorption measurements, we assume that not more than a few weight percent of CN−ether−PPV are distributed in the remaining layer.

On the basis of this result, we conclude that spin coating a CN−ether−PPV/M3EH−PPV blend does not lead to a uniform blend layer. We rather propose that a vertically composition gradient is formed with CN−ether−PPV excess at the top and a M3EH−PPV excess at the bottom as sketched in Figure 5.

First a layer of M3EH−PPV, containing a few percent of CN−ether−PPV, is formed when the solvent starts to evaporate and the relative polymer concentration increases. Then

---

(21) Morteani, A. C.; Dhoot, A. S.; Kim, J.-S.; Silva, C.; Greenham, N. C.; Murphy, C.; Moons, E.; Cina, S.; Burroughes, H.; Friend, R. H. *Adv. Mater.* **2003**, *15*, 1708−1712.

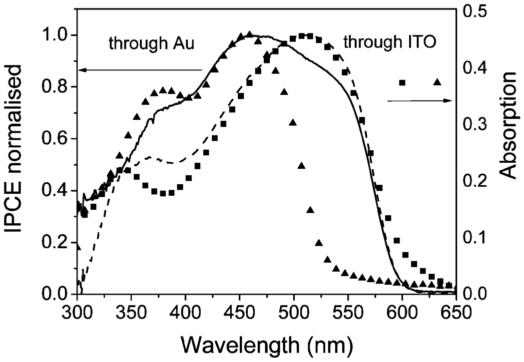

Figure 6. Normalized IPCE spectra for a device coated at 2400 rpm illuminated through the ITO substrate (dashed solid line) and through the Au top electrode (solid line). For comparison the absorption of a M3EH−PPV layer (squares) and of a CN−ether−PPV (triangles) are shown. The IPCE spectra were corrected by the transmission of the ITO/PEDOT or Au layer.

a second layer containing a blend of CN−ether−PPV and a minor (better soluble) fraction of M3EH−PPV is formed at increasing concentrations. Since the devices were illuminated from the ITO side and due to interference effects, more light is absorbed in the region close to the ITO, where M3EH is in excess. This leads to a pronounced contribution of M3EH−PPV in the IPCE spectra in the wavelength region around 500 nm.

A vertically segregated layer should also show characteristic differences in the shape of the IPCE spectrum when illuminated through the ITO or through the top electrode, as most photons are absorbed in the polymer layer close to the surface in face of an illumination source. Therefore, blend devices were prepared with a semitransparent 10 nm thick Au top electrode. Since the thin Au layer has only a small reflectivity, interference effects should be significantly suppressed which might otherwise influence the shape of the IPCE characteristics.[22] Obvious differences in the spectral shape of the IPCE characteristics are found (Figure 6). Whereas illumination through the ITO side resembles the M3EH−PPV absorption, the IPCE spectra upon illumination through the semitransparent Au electrode is rather identical to pure CN−ether−PPV absorption. A significant M3EH−PPV contribution can be identified only at longer wavelengths, where the CN−ether−PPV becomes less absorbent. The open-circuit voltage under white light illumination is 0.47 V if illuminated through ITO and around 0.4 V for illumination through the Au electrode, with the Au electrode always negative. Since the work functions of PEDOT and Au are comparable, the external electric field should be close to zero and the open-circuit voltage must be due to the diffusion current always present in bilayer devices.[10] Note that a solar cell incorporating a homogeneous blend as active layer and an energetically symmetric electrode configuration might generate a diffusion current and thus a nonzero open-circuit voltage, if one electrode collects predominantly one type of charge carrier or if the mobility of the charge carriers is unbalanced. However, an inversion of the open-circuit voltage under illumination from different sides is expected for a homogeneous blend and symmetric electrode configuration, due to symmetry considerations, in contrast to the results reported here. This underlines the scenario of formation of a graded bilayer structure.

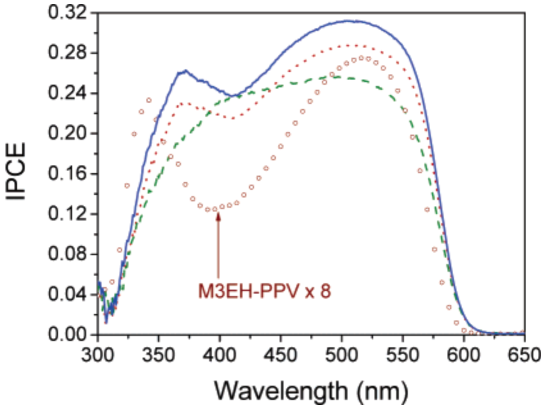

Figure 7. IPCE characteristics for bilayer devices consisting of a 25 nm thick M3EH−PPV layer followed by either a 23 nm (dotted) or a 33 nm (dashed) thick layer of CN−ether−PPV. For comparison the IPCE spectra of a single layer M3EH−PPV device and of the 55 nm thick M3EH−PPV:CN−ether−PPV 1:1 blend device (solid line) are shown.

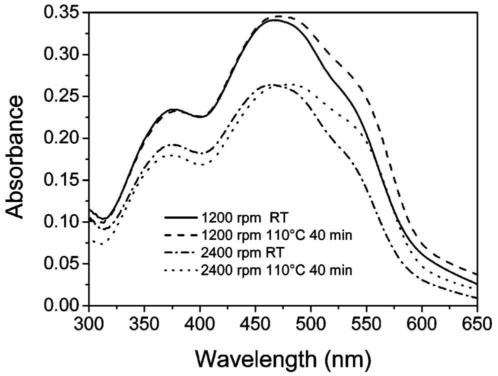

Figure 8. Absorbance of a blend of M3EH−PPV and CN−ether−PPV in a ratio of 1:1 for different spinning speeds as-prepared and after annealing at 110 °C for 40 min.

Overall, the proposed vertically composition graded structure is very close to an optimal geometry with respect to directional exciton separation at the interface and good transport of separated charges to the corresponding electrodes. It is well-known that this kind of structure will lead to improved efficiencies, but up to now these structures could only be realized by complicated laminating techniques.[7]

The fact, that the major M3EH−PPV fraction is mainly insoluble in xylene can be utilized for the direct construction of double-layer devices. Preparing first a pure M3EH−PPV layer by coating from a solution of the polymer in chlorobenzene, followed by the coating of a pure CN−ether−PPV layer from xylene leads to a double-layer structure. Therefore, the comparison of the photovoltaic characteristics of solar cells based on this well-defined double-layer structure with those described above should give further evidence for the proposed vertical phase separation in blend layers.

As shown in Figure 7, double-layer solar cells prepared by subsequent coating of a layer of M3EH−PPV followed by a layer of CN−ether−PPV show similar efficiencies and spectral characteristics compared to blend based devices. Intensity-dependent measurements did show the same linear behavior of the short-circuit current as presented for the blend

---

(22) Zen, A.; Neher, D.; Bauer, C.; Asawapirom, U.; Scherf, U.; Hagen, R.; Kostromine, S.; Mahrt, R. *Appl. Phys. Lett.* **2002**, *80*, 4699.

devices proving that double layers as well as blends are limited by the same kind of monomolecular recombination processes. The maximum peak efficiency of 28.8% was found for a device with the thinnest electron-acceptor layer. This device also exhibits the highest white light efficiency of 1.34%. For this device the shape of the spectrum of the double-layer device is similar to that of the blend device discussed earlier, again indicating that blend and double layers are of similar structure.

Increasing the CN−ether−PPV layer thickness from 23 nm to 33 nm leads to a decrease of the peak efficiency but to an increase of the absorption in the range near the peak absorption of CN−ether−PPV within 400−450 nm. From the low influence of the CN−ether−PPV thickness on the efficiency it can be concluded that the electron transport in CN−ether−PPV is quite well compared to other types of acceptors. In recent work on electron-accepting cyano-substituted PPE−PPV copolymers, we observed a significant influence of the thickness of the electron-acceptor layer on the absolute efficiency of double-layer devices in combination with M3EH−PPV.[23] In fact, for double-layer devices with a M3EH−PPV layer coated with CN−PPE−PPV, an increase in the CN−PPE−PPV layer thickness by 10 nm reduced the efficiency by a factor larger than 2.

No significant differences can be observed between the characteristics of blend and bilayer devices, and the thickness of the electron-accepting phase has only minor influence on the photovoltaic properties (Table 1). The open-circuit voltage was ca. 1.3 V for all devices and the fill factor varied only slightly between 30.6 and 32.4%, proving the assumption of good charge transport in the CN−ether−PPV layer. These values are similar to the values found for the blend devices.

Table 1. Overview of the Characteristic Parameters Obtained for M3EH−PPV Based Solar Cells

structure		V_{OC}, V	FF, %	IPCE, %	I_{SC}, mA	ECE, %
blend	1:1 M3EH−PPV:CN−ether−PPV	1.36	35.4	31	3.57	1.70
bilayer	M3EH−PPV:CN−ether−PPV	1.31	32.4	28	3.12	1.33

Conclusions

We reported on detailed studies on solar cells based on the alternating copolymer M3EH−PPV as electron donator and CN−ether−PPV as the electron-accepting component. We propose that due to the much lower solubility of M3EH in chlorobenzene compared to CN−ether−PPV, not a homogeneous blend but a vertically composition graded layer is formed during spin coating. This leads to a nearly ideal structure for thin layers facilitating both exciton separation and efficient transport of the separated charges to the corresponding electrodes in an efficient way. As a result, solar cells prepared from a blend of M3EH−PPV and CN−ether−PPV yield very high energy efficiencies of up to 1.7% under 100 mW/cm^2 white light irradiation.

Acknowledgment. We would like to thank the Volkswagen Stiftung for funding most of this work and the Verband der Chemischen Industrie for further financial support. We also thank Chunhong Yin and Elizabeth Lekha Paul for their technical support.

CM050148N

---

(23) Egbe, D. A. M.; Kietzke, T.; Carbonnier, B.; Mühlbacher, D.; Hörhold, H.-H.; Neher, D.; Pakula, T. *Macromolecules* **2004**, *37*, 8863−8873.